© 2023 Journal of Pharmacy & Pharmacognosy Research, 11 (1), 101-109, 2023
ISSN 0719-4250
https://jppres.com

DOI: https://doi.org/10.56499/jppres22.1529_11.1.101

Original Article

Bioadsorption of silver ions by calcareous chitin, chitin and chitosan

[Bioadsorción de iones de plata por quitina calcárea, quitina y quitosano]

John Jáuregui-Nongrados[1], Angel T. Alvarado[2*], Miguel Mucha[1], Ana M. Muñoz[3], Haydee Chávez[4], Aura Molina-Cabrera[4], Pompeyo A. Cuba-García[4], Elizabeth J. Melgar-Merino[4], Mario Bolarte-Arteaga[5], Jaime A. Mori-Castro[6]

[1]Environmental Engineering, San Ignacio de Loyola University, La Molina 15024, Lima, Peru.
[2]International Research Network of Pharmacology and Precision Medicine (REDIFMEP), San Ignacio de Loyola University, La Molina 15024, Lima, Peru.
[3]Institute of Food Science and Nutrition, ICAN, San Ignacio de Loyola University, La Molina 15024, Lima, Peru.
[4]Faculty of Pharmacy and Biochemistry, San Luis Gonzaga National University of Ica, 11004, Ica, Peru.
[5]Human Medicine, Continental University, Los Olivos 15304, Lima, Peru.
[6]Professional School of Nursing, Faculty of Health Sciences, Norbert Wiener University, Lince 15046, Lima, Peru.
*E-mail: angel.alvarado@usil.pe

Abstract

Context: Calcareous chitin, chitin, chitosan, and their modifications are used as bioadsorbents of metals and dyes that cause environmental pollution, endocrine disruption, and human diseases.

Aims: To evaluate the selective bioadsorption of silver ions (Ag^+) by calcareous chitin, chitin, and chitosan.

Methods: Experimental and prospective study. The presence of functional groups of the bioadsorbents was identified by Fourier-transformed infrared spectroscopy (FT-IR), ^{1}H-NMR spectroscopy and scanning electron microscopy (SEM). The Langmuir, Freundlich, and Elovich models were applied to describe the adsorption capacity of bioadsorbents according to granule size (20-40, 40-60, 60-80 meshes) and temperature (10, 20, and 30°C).

Results: The FT-IR spectrum of calcareous chitin indicates the presence of carbonate ($CO_3^=$ 1420 cm^{-1}), amide III (1313 cm^{-1}), –OH groups (3441.90 cm^{-1}), and pyranose structure (952.83 cm^{-1}); chitin has –OH groups (3441.90 cm^{-1}), NH (3268 cm^{-1}), amide I (1654 cm^{-1}) and II (1559 cm^{-1}); chitosan has –OH groups (3419.90 cm^{-1}), –NH (3200 cm^{-1}), amide I (1712.18 cm^{-1}), $-NH_2$ (1654.46 cm^{-1}), amide III (1317.11 cm^{-1}) and pyranose structure (1070.12 cm^{-1} and 1031 cm^{-1}). The Langmuir model indicates greater bioadsorption of Ag^+ ions at smaller particle sizes (60-80 = 0.25-0.18 mm) and at a temperature of 20-30°C.

Conclusions: The bioadsorption of silver ions (Ag^+) by chitosan is greater with respect to calcareous chitin and chitin; the Langmuir model fits for the Ag^+ isotherm and suggests that the process is controlled by physisorption.

Keywords: bioadsorption; calcareous chitin; chitin; chitosan; silver ions.

Resumen

Contexto: La quitina calcárea, quitina, quitosano y sus modificaciones se utilizan como bioadsorbentes de metales y tintes causantes de la contaminación medioambiental, disrupción endocrina y enfermedades en humanos.

Objetivos: Evaluar la bioadsorción selectiva de iones plata (Ag^+) por quitina calcárea, quitina y quitosano.

Métodos: Estudio experimental y prospectivo. Se identificó la presencia de grupos funcionales de los bioadsorbentes por espectroscopia infrarroja transformada de Fourier (FT-IR), espectroscopia ^{1}H-RMN y por microscopía electrónica de barrido (SEM). Se aplicó los modelos de Langmuir, Freundlich, y Elovich, para describir la capacidad de adsorción de los bioadsorbentes de acuerdo al tamaño del granulo (20-40, 40-60, 60-80 meshes) y temperatura (10, 20 y 30°C).

Resultados: El espectro FT-IR de la quitina calcárea indica presencia de carbonato ($CO_3^=$ 1420 cm^{-1}), amida III (1313 cm^{-1}), grupos –OH (3441,90 cm^{-1}) y estructura piranósica (952,83 cm^{-1}); quitina presenta grupos –OH (3441,90 cm^{-1}), NH (3268 cm^{-1}), amida I (1654cm^{-1}) y II (1559 cm^{-1}); quitosano se identifica grupos –OH (3419.90 cm^{-1}), –NH (3200 cm^{-1}), amida I (1712.18 cm^{-1}), $-NH_2$ (1654.46 cm^{-1}), amida III (1317.11 cm^{-1}) y estructura piranósica (1070.12 cm^{-1} y 1031 cm^{-1}). El modelo de Langmuir indica mayor bioadsorción de iones Ag^+ a menor tamaño de partícula (60-80 = 0.25-0.18 mm) y a una temperatura de 20-30°C.

Conclusiones: La bioadsorción de iones de plata (Ag^+) por quitosano es mayor respecto a quitina calcárea y quitina; el modelo de Langmuir se ajusta para la isoterma de Ag^+ y sugiere que el proceso está controlado por fisisorción.

Palabras Clave: bioadsorción; iones plata; quitina; quitina calcárea; quitosano.

ARTICLE INFO
Received: Octubre 24, 2022.
Accepted: December 24, 2022.
Available Online: January 2, 2023.

AUTHOR INFO
ORCID: 0000-0002-7252-2591 (JJN) 0000-0002-8717-4307 (HC) 0000-0001-9939-8917 (MBA)
0000-0001-8694-8924 (ATA) 0000-0001-7953-4168 (AMC) 0000-0003-2570-0401 (JAMC)
0000-0003-3449-2210 (MM) 0000-0002-0468-154X (PACG)
0000-0003-3080-9823 (AMM) 0000-0002-9033-8042 (EJMM)

INTRODUCTION

Nanomaterials are small structures of 1 µm in diameter used in different research sciences (Kumar et al., 2022). Especially in bionanotechnology, metallic nanoparticles with a size smaller than a human cell are used (Basova et al., 2021; Oliver and Oliver, 2017). Silver nanoparticles (Ag NP) and other biocompatible metals are used as diagnostic biomarkers, implants, delivery systems and drug transporters, and as drugs for their potential anticancer and anti-inflammatory activity (Basova et al., 2021; Mousavi et al., 2018; Oliver and Oliver, 2017; Soto-Vazquez et al., 2022), and due to its antimicrobial and antiviral activity, personal protective equipment against COVID-19 has been designed (Sportelli et al., 2020). Additionally, it is used as catalysts and degraders of various substances such as dyes (Kumar et al., 2022). Various reducing agents are used in the synthesis of AgNP, such as ascorbate (C_6H_7 NaO_6), sodium borohydride ($NaBH_4$), sodium citrate ($Na_3C_6H_5O_7$), dextrose ($C_6H_{12}O_6$), ethylene glycol ($C_2H_6O_2$), hydrogen, hydrazine (N_2H_4), hydrate hydrazine (N_2H_4-NH_2•H_2O), N-dimethylformamide (DMF) (Goulet and Lennox, 2010; Lee and Jun, 2019), additionally, silver ions (Ag^+), and the residues of the aforementioned reducing agents are emitted in the effluents of these industries (Wang et al., 2020). Nanoparticles are likely to induce kidney, blood, and liver dysfunction in humans, while Ag^+ ions and AgNP synthesis residues are responsible for endocrine disruption in various animal species (Kumar et al., 2022; Mousavi et al., 2018; Wang et al., 2020).

In this sense, the effective extraction and recovery of Ag^+ ions from waste sources are of concern (Golnaraghi Ghomi et al., 2020), for which various methods have been designed, such as chemical precipitation, ion exchange, electrodialysis, solvent extraction and reverse osmosis (Ding et al., 2019; Gao et al., 2013; Zhao et al., 2020). These techniques are complex, with low selectivity, high operating and capital costs, and at the same time, generate large amounts of secondary waste (Hsu et al., 2019). For this reason, a green research line of nanoparticles has been proposed that are chemically stable and of low toxicity to the environment (Kumar et al., 2022), biocompatible, inert to tissues, non-carcinogenic, have sufficient mechanical resistance and be resistant to the influence of the internal environment of the human organism (Basova et al., 2021); and within this line, the use of natural products with chelating or bioadsorption capacity, low cost, sustainable over time and with minimal impact on the environment has been proposed as an alternative (Petrova et al., 2015). Being chitin a renewable biopolymer with adsorption capacity that is obtained from the exoskeleton of the *Penaeus* sp. and *Carcinus maenas* (crab) (Jiang et al., 2017); and from the aforementioned biopolymer, chitosan (poly-β-(1→4)-2-amino-2-deoxy-D-glucose) is obtained, which is a macromolecular structure with amino groups (-NH_2) and hydroxyl (-OH) efficient to chelate or adsorb metal ions, at the same time, they meet the requirements of the green line, for being biocompatible, biodegradable, non-toxic and of low economic cost to be used in countries with emerging economies (Pascu et al., 2020).

After conducting a review in the PubMed ScienceDirect database on metal adsorption studies with calcareous chitin, chitin and chitosan in Peru, it has been shown that studies using this method are scarce, so it is worth studying these biopolymers, make scientific evidence of its properties of bioadsorption of potentially toxic metals for the environment and for public health. Therefore, the objective was to evaluate the selective bioadsorption of silver ions (Ag^+) by calcareous chitin, chitin, and chitosan.

MATERIAL AND METHODS

Type of study

An experimental and prospective study was carried out from January to September 2022.

Chemical reagents

All solvents and reagents were of analytical grade and ACS (American Chemical Society) quality purchased from Mercantil Laboratorio SAC (Lima, Peru): hydrochloric acid (HCl), sulfuric acid (H_2SO_4), sodium hydroxide (NaOH), sodium sulfite (Na_2SO_3) and silver nitrate ($AgNO_3$). Calcareous chitin, chitin, and chitosan were used with degrees of deacetylation of 35.91, 35.55, and 76.4%, respectively, and with a particle size of 20-40, 40-60, and 60-80 meshes according to the Tyler series.

Obtaining the bioadsorbents

To remove proteins and obtain calcareous chitin from the shrimp exoskeleton, a sufficient quantity of sodium hydroxide (NaOH) 10% ($^w/_w$) was added and left to stand for 2 h at room temperature; after that time, it was filtered to obtain the solid phase, which was washed with distilled water until obtaining a solid product of calcareous chitin at pH 7. Subsequently, a quantity of calcareous chitin was treated with 10% ($^v/_v$) hydrochloric acid (HCl) for 15 min to remove the minerals from the calcareous biopolymer; then, it was filtered to obtain the chitin solid. This solid was washed with distilled water until pH 7.

Finally, the chitin was treated with NaOH 50% ($^{w}/_{w}$) for 1 h at 120°C, obtaining the chitosan, which was washed with distilled water until pH 7, then filtered and the solid dried in an oven at 50°C (Binder, ED-23 1107209, Germany) for 12 h (Khayrova et al., 2021; Pavlova and Trusova, 2021).

Preparation of silver ion solutions with bioadsorbents

A sufficient quantity of silver nitrate ($AgNO_3$) was weighed to obtain a stock solution of 1000 ppm of silver ions (Ag^+); then, solutions of 10, 20, 30, 50, 100, and 200 ppm of Ag^+ ions at pH 4 were prepared; 100 mg of each study bioadsorbent was added to these solutions. These samples were used to quantify Ag^+ ions and to carry out isothermal studies of natural bioadsorbents.

Quantification method and characterization of biosorbents

The silver ions (Ag^+) of the aqueous solution were quantified by the flame atomic absorption spectrometry method (FAAS), using a Perkin-Elmer model 2500, USA, equipment equipped with a silver hollow cathode lamp with an air-acetylene flame. Samples were read at a wavelength of 328.1 nm (Sergeevna et al., 2020; Terzioğlu et al., 2021).

Polymeric bioadsorbents were characterized by scanning electron microscopy (SEM), ^{1}H-NMR spectroscopy, and Fourier Transform Infrared Spectroscopy (FTIR) to identify and confirm the functional groups present while observing the surface morphology of each biopolymer (Sharef and Fakhre, 2022; Weißpflog et al., 2021).

Effect of granulometry on biosorption isotherms

To evaluate the effect of granulometry, 50 mL of solutions of 10, 20, 30, 50, 100, and 200 ppm of Ag^+ ions at pH 4 were previously prepared from the stock solution (1000 ppm Ag^+); 100 mg of each study bioadsorbent (20-40, 40-60 and 60-80 mesh) was added to these solutions, then it was placed in a thermostatic bath at 20°C with constant stirring for 2 h (IKA Shaker, C-MAG HS7, Germany). Subsequently, 5 mL samples were taken to determine the amount of metal retained on the bioadsorbent surface. The amount of metal retained by the bioadsorbent was calculated using the following equation [1] (Pascu et al., 2020).

$$q = \frac{(C_i - C_{eq})}{m} V \quad [1]$$

Where: C_i is the initial concentration of metal ions in solution, C_{eq} is the concentration of metal ions in the solution after reaching equilibrium in the complexing reaction, V is the volume of the solution used, and "m" is the mass of the bioadsorbent used.

Effect of temperature on biosorption isotherms

To determine the effect of temperature on the Ag^+ ion chelation process by the bioadsorbents, solutions of the adsorbent polymers were previously prepared at a final concentration of 2 mg/mL; then 50 mL of solutions of 10, 20, 30, 50, 100 and 200 ppm of Ag^+ ions were added. The resulting solution was stirred for 2 h at temperatures of 10, 20, and 30°C. The solutions of each temperature were filtered and read at a wavelength of 328.1 nm in the flame atomic absorption spectrophotometer (FAAS, Perkin-Elmer model 2500, USA) (Banisheykholeslami et al., 2021).

Desorption process

To study the desorption process, 100 mg of chitosan Ag^+ ions were weighed (in a beaker), then 20 mL of 0.1 M H_2SO_4 or 0.1 M Na_2SO_3 were added, as the case may be, and kept under constant agitation (IKA shaker, C-MAG HS7, Germany) for 90 min, during the shaking time samples were taken at different times. The solutions were filtered and then diluted for reading in the flame atomic absorption spectrophotometer (FAAS, Perkin-Elmer model 2500, USA) (Sadiq et al., 2020; Mao et al., 2020).

Statistical analysis

The experimental results were analyzed and validated using the Langmuir and Freundlich isotherm models, and the Elovich kinetic model to describe the ion (Ag+) bioadsorption capacity. Studies were performed in triplicate, data were expressed as arithmetic mean ± standard deviation (SD), and the one-factor analysis of variance (ANOVA) was applied. A value of $p<0.05$ was considered statistically significant. The GraphPad Prism 9 version 9.1.2 Statistical Software was used.

RESULTS AND DISCUSSION

Fig. 1A shows the FT-IR infrared spectroscopy of natural bioadsorbents. In the FT-IR spectrum of calcareous chitin a higher intensity signal (1420 cm^{-1}) is observed with respect to chitin, due to the presence of carbonate ($CO_3^=$), the absorption 1313 cm^{-1} indicates the presence of amide III, 1073 cm^{-1} corresponds to the tension of CO, and 952.83 cm^{-1} corresponds to the vibration of the pyranose structure. Fig. 1B shows the FT-IR spectrum of chitin, which presents an absorption band of 3441.90 cm^{-1} corresponding to –OH groups, as observed in calcareous chitin, the band 3268 cm^{-1} corresponds to the tension of NH; while bands 1654 and 1559 cm^{-1} correspond to amide I and II bands that are characteristic of chitin. Fig. 1C shows the FT-IR spectrum of chitosan, where absorption spectra are identified: 3419.90 cm^{-1} for -OH groups,

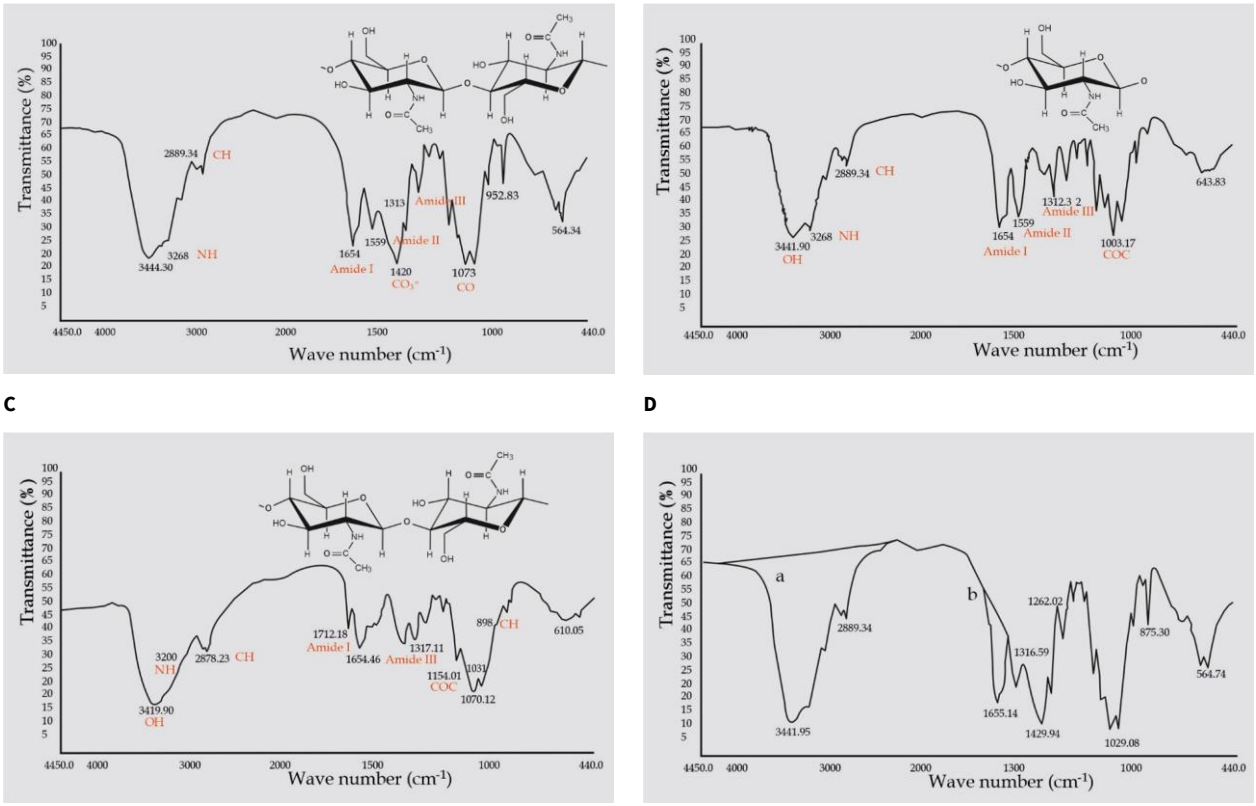

Figure 1. FT-IR infrared spectroscopy of natural bioadsorbents.

(A) Infrared spectrum of calcareous chitin; **(B)** chitin; **(C)** chitosan; and **(D)** infrared spectrum of the calcareous chitin and the baseline are observed to evaluate the degree of acetylation (GA).

3200 cm^{-1} for -NH group, the same one that is increased with respect to chitin after the deacetylation process, at 2878.23 cm^{-1} the CH tension; the amide I band appears at 1712.18 cm^{-1} due to the increase in the intensity of the amino groups, while it is associated with acetamide residues after deacetylation; absorption 1654.46 cm^{-1} corresponds to the doublet of the $-NH_2$ group, 1317.11 cm^{-1} corresponds to amide III, while the amide II band practically disappears. The absorption 1154.01 cm^{-1} is attributed to the asymmetric strain of the C-O-C group, 1070.12 cm^{-1} and 1031 cm^{-1} are vibrations of the pyranose structure. Fig. 3D shows the absorbances of calcareous chitin and the trace of the baseline to calculate the absorbances at 1655 and 3456 cm^{-1}, and with this, the degree of acetylation (GA) of the sample was evaluated: GA= 115 $[(A_{1655}/A_{3456})]$; and its acetylation percentage was 64.45%.

Fig. 2A shows the absorbances of the chitin and the trace of the baseline to calculate the absorbances that allow evaluating the GA of the sample; the percentage of acetylation of this biopolymer was 64.09%, with respect to calcareous chitin, there is no marked difference, despite the high content of carbonates in calcareous chitin. The FT-IR method was used to evaluate the GA of solid samples of calcareous chitin and chitin, since they are not soluble in most solvents, and it is not feasible to determine the GA by NMR. Fig. 2B shows the ratio of intensities of the protons (hydrogen ions) H_1D (1.000), H_1A (0.349), H_2D (1.061) and CH_3 (0.858) of chitosan by the ^{1}H-NMR method. This technique was used since it does not require a high sample concentration. There was no interference between the selected signals and even combining them to evaluate the GA of this biopolymer. GA is a physicochemical property that influences the metal bioadsorption capacity of chitosan, which is determined by the areas of the proton peaks: $\%GA = [(H_1A + CH_3/3)/(H_1D + H_1A + H_2D + CH_3/3)].100$; whose %GA was 23.55%, and the degree of deacetylation (GD) value was 76.45%, being classified as chitosan with medium GD. In the study by Azizkhani et al. (2021), the FT-IR method and others (TEM, Zeta potential, and XRD analysis) were used to characterize the structure of graphene oxide with silica and chitosan. In another study, El-Naggar et al. (2022) inferred the chemical structure of chitosan nanoparticles (CsNPs) by FT-IR, ^{1}H-NMR, and ^{13}C-NMR.

Fig. 3 shows the scanning electron microscopy (SEM) of the calcareous chitin (Fig. 3A), in which a

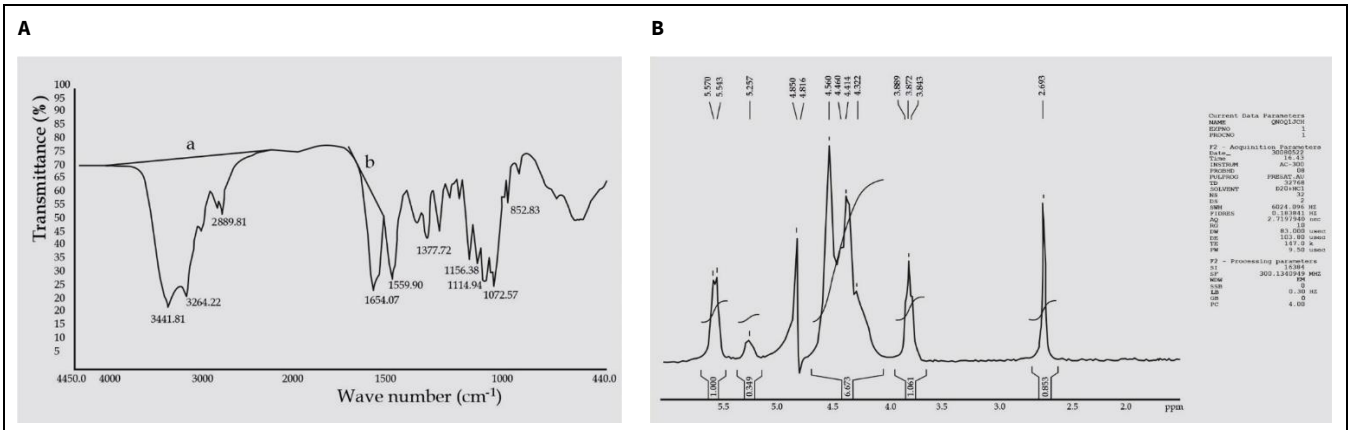

Figure 2. Infrared FT-IR spectroscopy of the chitin bioadsorbent to evaluate the degree of acetylation (GA) and intensity of the protons.

(A) Infrared spectrum of the chitin and the trace of the base line to calculate the absorbances that allow the evaluation of the GA; **(B)** ratio of intensities of the protons H_1D (1.000), H_1A (0.349), H_2D (1.061) and CH_3 (0.858) of chitosan by the ^{1}H-NMR method.

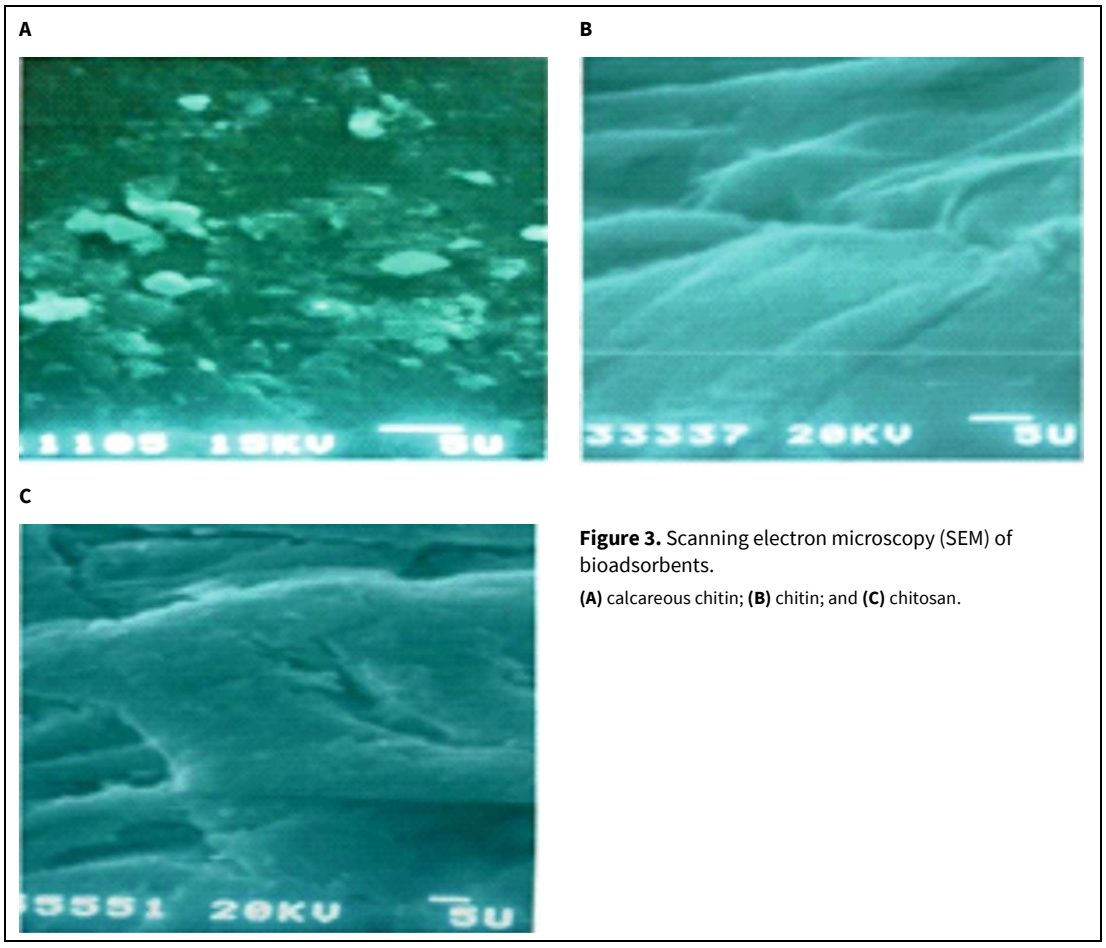

Figure 3. Scanning electron microscopy (SEM) of bioadsorbents.

(A) calcareous chitin; **(B)** chitin; and **(C)** chitosan.

rough surface is observed, due to the high content of carbonates, while chitin (Fig. 3B) has overlapping layers with a more homogeneous surface. It is also noted that the surface of chitosan (Fig. 3C) consists of overlapping layers, somewhat less rough than calcareous chitin.

The experimental results were analyzed and validated using the Langmuir and Freundlich isotherm models and the Elovich kinetic model to describe the ion bioadsorption capacity (Ag^+). Table 1 shows the bioadsorption isotherms using different particle sizes of the three types of bioadsorbents. It can be seen that in all the adsorption isotherms, the size of the granule influences, with the bioadsorption of Ag^+ ions being greater at a size of 60-80 mesh diameter (0.25-0.18 mm); and comparing the three bioadsorbents, the most efficient is chitosan. The analysis of the correlation coefficient shows that the Freundlich model is

Table 1. Adsorption parameters of natural bioadsorbents according to granulometry and Langmuir, Freundlich, and Elovich models.

Bioadsorbente	Mesh size*	Langmuir parameters			Freundlich parameters			Elovich parameters		
		q_m (mg/g) Mean ± SD	b (L/mg) Mean ± SD	R^2	K Mean ± SD	1/n Mean ± SD	R^2	K_E (L/mg) Mean ± SD	q_m (mg/g) Mean ± SD	R^2
Calcareous chitin	20-40	39.69 ± 0.44	0.03 ± 0.01	0.89	2.73 ± 0.25	0.51 ± 0.06	0.99	0.11 ± 0.04	16.11 ± 0.41	0.84
	40-60	44.82 ± 0.29	0.04 ± 0.01	0.87	3.77 ± 0.18	0.49 ± 0.10	0.97	0.16 ± 0.05	17.60 ± 0.61	0.81
	60-80	46.51 ± 0.45	0.04 ± 0.01	0.85	3.87 ± 0.16	0.50 ± 0.04	0.96	0.14 ± 0.05	19.50 ± 0.61	0.76
Chitin	40-60	19.46 ± 0.29	0.03 ± 0.01	0.85	3.34 ± 0.07	0.33 ± 0.03	0.97	0.26 ± 0.04	5.99 ± 0.49	0.65
	60-80	21.55 ± 0.32	0.05 ± 0.03	0.93	3.90 ± 0.08	0.31 ± 0.01	0.98	0.74 ± 0.04	5.35 ± 0.38	0.82
Chitosan	20-40	65.36 ± 0.72	0.19 ± 0.03	0.88	13.46 ± 0.09	0.37 ± 0.03	0.93	2.19 ± 0.10	17.24 ± 0.50	0.80
	40-60	68.96 ± 0.95	0.39 ± 0.08	0.87	22.19 ± 0.08	0.27 ± 0.02	0.95	27.55 ± 0.48	11.99 ± 0.22	0.77
	60-80	72.46 ± 0.70	0.53 ± 0.05	0.86	25.53 ± 0.20	0.28 ± 0.02	0.92	38.43 ± 0.45	12.82 ± 0.13	0.77

*Mesh 20-40 = 0.8-0.42 mm; mesh 40-60 = 0.42-0.25 mm; mesh 60-80 = 0.25-0.18 mm. q_m: Maximum solute bioadsorption capacity, in the monolayer (mg/g); b: Langmuir or affinity energy constant (L/mg); K: adsorption energy function; 1/n: adsorption intensity; K_E: Elovich equilibrium constant (L/mg); SD: Standard deviation. The analysis of variance (ANOVA) for the adsorption parameters of natural bioadsorbents according to granulometry and models shows that the difference in means is statistically significant ($p<0.05$; 0.0003 calcareous chitin, 0.005 chitin, and 0.00003 chitosan).

more efficient for the bioadsorption of Ag^+ ions; the adsorption energy function (K) values increase as a function of the decrease in adsorbent particle size, which reaffirms that the adsorption capacity of bioadsorbents increases as their size decreases; the values of adsorption intensity (1/n) are in the range of 0.1-1.0 for the three sizes of bioadsorbents, indicating that adsorption is favorable in all cases. Al-Wabel et al. (2021) used the models of Langmuir, Freundlich, Redlich-Peterson, and Temkin to determine the adsorption parameters of chitosan-BC (CBC) microsphere beads. Azizkhani et al. (2021) validated the results of adsorption of graphene oxide with silica and chitosan with the models of Langmuir, Freundlich, Temkin, Harkins-Jura and Dubinin-radushkevich. They showed that the Langmuir, Freundlich, and Temkin models fit well for cadmium ion (Cd^{2+}) removal. Using the Langmuir model, the maximum adsorption capacity (126.58 mg/g) of the modified adsorbent was determined. El-Naggar et al. (2022) used the model of Langmuir, Freundlich, and Elovich to evaluate the adsorption of synthetic dyes and trace metals simultaneously from chitosan nanoparticles (CsNP); the adsorption of the synthetic dye followed the Langmuir model, while the adsorption of the lead ion (Pb^{2+}) followed the Freundlich and Elovich model.

Table 2 describes the adsorption parameters of natural bioadsorbents according to temperature and according to the Langmuir, Freundlich, and Elovich models. The analysis of the three experimental temperatures shows that the Freundlich model also better describes the process. The K values increase as the temperature of the solution increases, the optimum being between 20-30°C; the values of 1/n are between 0.1-1.0 for the three temperatures, indicating that bioadsorption is favorable. Analyzing the maximum solute bioadsorption capacity (q_m) of Langmuir in all the experiments, varying the size of the bioadsorbent or the temperature, it is observed that chitosan has a greater adsorption capacity for Ag^+ ions, followed by calcareous chitin.

Based on the results of the three bioadsorbents (calcareous chitin, chitin and chitosan), it has been verified that chitosan shows greater adsorption and/or chelation capacity, therefore, for the Ag^+ desorption study, chitosan (0.42-0.25 mm), 0.1 M H_2SO_4 and 0.1 M Na_2SO_3 were used; and the percentage of desorption was determined at 10, 20, 30, 40, 50, 60, 70, 80 and 90 min. At 10 min, desorption was determined to be 73% and 86% for H_2SO_4 and Na_2SO_3, respectively. And after 60 min, practically 82 and 92% are recovered in each case, which indicates that the desorption and adsorption of Ag^+ are fast and efficient processes. In a previous study, Petrova et al. (2015) explain that the sulfo groups of N-(2-sulfoethyl)-chitosan are efficient in selectively adsorbing copper (Cu^{2+}) and silver (Ag^+) ions from complex solutions. The selectivity coefficient KAg/Cu increased to 20 (ammonium acetate buffer solution pH 6.5) with an increase in the degree of sulfoethylation of the adsorbent to 1.0. Li et al. (2020) have shown that silver chloride-modified chitosan trapped in cross-linked chitosan microspheres (AgCl@CM) are excellent adsorbents of iodide anions found in wastewater. Al-Wabel et al. (2021) showed that chitosan-BC microsphere beads (CBC) remove 16.2-25.6% more sulfathiazole (STZ) from contaminated aqueous media than other bioadsorbents.

Table 2. Adsorption parameters of natural bioadsorbents according to temperature and the Langmuir, Freundlich and Elovich models

Bioadsorbente	T°	Langmuir parameters			Freundlich parameters			Elovich parameters		
		q_m (mg/g) (Mean ± SD)	b (L/mg) (Mean ± SD)	R^2	K (Mean ± SD)	1/n (Mean ± SD)	R^2	K_E (L/mg) (Mean ± SD)	q_m (mg/g) (Mean ± SD)	R^2
Calcareous chitin	10	39.68 ± 0.17	0.03 ± 0.01	0.84	1.57 ± 0.10	0.34 ± 0.02	0.91	0.19 ± 0.02	16.39 ± 0.10	0.69
	20	44.24 ± 0.15	0.04 ± 0.02	0.87	3.35 ± 0.03	0.33 ± 0.02	0.93	0.18 ± 0.01	17.60 ± 0.20	0.82
	30	49.51 ± 0.35	0.05 ± 0.01	0.88	3.64 ± 0.03	0.12 ± 0.01	0.91	0.22 ± 0.02	18.51 ± 0.12	0.78
Chitin	10	17.66 ± 0.13	0.02 ± 0.01	0.81	1.57 ± 0.06	0.37 ± 0.02	0.81	0.19 ± 0.03	6.94 ± 0.08	0.59
	20	20.87 ± 0.10	0.03 ± 0.01	0.80	1.99 ± 0.22	0.34 ± 0.02	0.91	0.18 ± 0.02	7.14 ± 0.03	0.60
	30	24.39 ± 0.10	0.03 ± 0.01	0.80	3.36 ± 0.18	0.33 ± 0.01	0.93	0.22 ± 0.01	8.06 ± 0.04	0.64
Chitosan	10	68.49 ± 0.39	0.33 ± 0.04	0.88	18.18 ± 0.04	0.30 ± 0.04	0.91	61.07 ± 0.03	10.89 ± 0.14	0.79
	20	68.97 ± 0.28	0.38 ± 0.02	0.87	20.08 ± 0.04	0.25 ± 0.02	0.93	27.96 ± 0.12	11.93 ± 0.08	0.77
	30	70.42 ± 0.11	0.44 ± 0.03	0.88	22.88 ± 0.02	0.24 ± 0.03	0.94	8.51 ± 0.18	14.28 ± 0.09	0.79

T°:Temperature; q_m: Maximum solute bioadsorption capacity, in the monolayer (mg/g); b: Langmuir or affinity energy constant (L/mg); K: adsorption energy function; 1/n: adsorption intensity; K_E: Elovich equilibrium constant (L/mg); SD: Standard deviation.

The analysis of variance (ANOVA) for the adsorption parameters of natural biosorbents according to temperature and models shows that the difference in means is statistically significant ($p<0.05$; 0.0007 calcareous chitin, 0.002 chitin, and 0.000001 chitosan).

The results of this study must be considered with the limitation of the sample, which was a solution of known concentration of silver ions (Ag^+) prepared from silver nitrate ($AgNO_3$). Therefore, in later studies, it is being considered to carry out an investigation with wastewater samples from Andean areas of Peru that extract silver; another limitation is not having compared bioadsorbents with other biopolymers used as metal removers. Notwithstanding the foregoing, these findings will form part of the scientific literature within the green or natural line for the removal of heavy metals and dyes from wastewater, whose purpose is to reduce environmental pollution, reduce endocrine dysfunction in mollusks and mitigate diseases generated by free radicals (Murcia-Salvador et al., 2019).

CONCLUSION

According to the results, it is concluded that the bioadsorption of silver ions (Ag^+) by chitosan is greater with respect to calcareous chitin and chitin. The Langmuir model fits for the Ag^+ isotherm and suggests that the process is mainly controlled by physisorption (weak adsorbate-adsorbent interaction forces). Scanning electron microscopy (SEM), ^{1}H-NMR spectroscopy, and Fourier Transformed Infrared (FT-IR) spectroscopy analysis of bioadsorbents show the presence of hydroxyl and amino groups that are involved in adsorption.

CONFLICT OF INTEREST

The authors declare no conflicts of interest.

ACKNOWLEDGMENTS

The authors thank the members of the Molecular Pharmacology Society of Peru for their participation in this study. This research did not receive any specific grant from funding agencies in the public, commercial, or not-for-profit sectors.

REFERENCES

Al-Wabel MI, Ahmad M, Usman ARA, Al-Farraj ASF (2021) Designing chitosan based magnetic beads with *Conocarpus* waste-derived biochar for efficient sulfathiazole removal from contaminated water. Saudi J Biol Sci 28(11): 6218–6229. https://doi.org/10.1016/j.sjbs.2021.06.072

Azizkhani S, Hussain SA, Abdullah N, Ismail MHS, Mohammad AW (2021) Synthesis and application of functionalized Graphene oxide-silica with chitosan for removal of Cd (II) from aqueous solution. J Environ Health Sci Eng 19(1): 491–502. https://doi.org/10.1007/s40201-021-00622-z

Banisheykholeslami F, Hosseini M, Najafpour Darzi G (2021) Design of PAMAM grafted chitosan dendrimers biosorbent for removal of anionic dyes: Adsorption isotherms, kinetics and thermodynamics studies. International J Biol Macromol 177: 306–316. https://doi.org/10.1016/j.ijbiomac.2021.02.118

Basova TV, Vikulova ES, Dorovskikh SI, Hassan A, Morozova NB (2021) The use of noble metal coatings and nanoparticles for the modification of medical implant materials. Maters Des 204: 109672. https://doi.org/10.1016/j.matdes.2021.109672

Ding Y, Zhang S, Liu B, Zheng H, Chang C, Ekberg C (2019) Recovery of precious metals from electronic waste and spent catalysts: A review. Resour Conserv Recycl 141: 284–298. https://doi.org/10.1016/j.resconrec.2018.10.041

El-Naggar ME, Radwan EK, Rashdan HRM, El-Wakeel ST, Koryam AA, Sabt A (2022) Simultaneous removal of Pb^{2+} and direct red 31 dye from contaminated water using N-(2-hydroxyethyl)-2-oxo-2H-chromene-3-carboxamide loaded chitosan nanoparticles. RSC Adv 12(29): 18923–18935. https://doi.org/10.1039/D2RA02526D

Gao Y, Zhou Y, Wang H, Lin W, Wang Y, Sun D, Hong J, Li, Q (2013) Simultaneous silver recovery and cyanide removal from electroplating wastewater by pulse current electrolysis using static cylinder electrodes. Ind Eng Chem Res 52(17): 5871–5879. https://doi.org/10.1021/ie301731g

Golnaraghi Ghomi A, Asasian-Kolur N, Sharifian S, Golnaraghi A (2020) Biosorpion for sustainable recovery of precious metals from wastewater. J Environ Chem Eng 8(4): 103996. https://doi.org/10.1016/j.jece.2020.103996

Goulet PJG, Lennox RB (2010) New insights into Brust−Schiffrin metal nanoparticle synthesis. J Am Chem Soc 132: 9582–9584. https://doi.org/10.1021/ja104011b

Hsu E, Barmak K, West AC, Park AHA (2019) Advancements in the treatment and processing of electronic waste with sustainability: A review of metal extraction and recovery technologies. Green Chem 21(5): 919–936. https://doi.org/10.1039/C8GC03688H

Jiang Y, Fu C, Wu S, Liu G, Guo J, Su Z (2017) Determination of the deacetylation degree of chitooligosaccharides. Mar Drugs 15(11): 332. https://doi.org/10.3390/md15110332

Khayrova A, Lopatin S, Varlamov V (2021) Obtaining chitin, chitosan and their melanin complexes from insects. Int J of Biol Macromol 167: 1319–1328. https://doi.org/10.1016/j.ijbiomac.2020.11.086

Kumar D, Niraula P, Aryal H, Budhathoki B, Phuyal S, Marahatha R, Subedi K (2022) Plant-mediated green synthesis of Ag NPs and their possible applications: A critical review. J Nanotechnol 2022: 2779237. https://doi.org/10.1155/2022/2779237

Lee SH, Jun BH (2019) Silver nanoparticles: Synthesis and application for nanomedicine. Int J Mol Sci 20(4): 865. https://doi.org/10.3390/ijms20040865

Li Q, Mao Q, Li M, Zhang S, He G, Zhang W (2020) Cross-linked chitosan microspheres entrapping silver chloride via the improved emulsion technology for iodide ion adsorption. Carbohydr Polym 234: 115926. https://doi.org/10.1016/j.carbpol.2020.115926

Mao J, Lin S, Lu XJ, Wu XH, Zhou T, Yun YS (2020) Ion-imprinted chitosan fiber for recovery of Pd(II): Obtaining high selectivity through selective adsorption and two-step desorption. Environ Res 182: 108995. https://doi.org/10.1016/j.envres.2019.108995

Mousavi SM, Hashemi SA, Ghasemi Y, Atapour A, Amani AM, Savar Dashtaki A, Babapoor A, Arjmand O (2018) Green synthesis of silver nanoparticles toward bio and medical applications: Review study. Artif Cells Nanomed Biotechnol 46(Supp. 3): S855–S872. https://doi.org/10.1080/21691401.2018.1517769

Murcia-Salvador A, Pellicer JA, Fortea MI, Gómez-López VM, Rodríguez-López MI, Núñez-Delicado E, Gabaldón JA (2019) Adsorption of direct blue 78 using chitosan and cyclodextrins as adsorbents. Polymers 211(6): 1003. https://doi.org/10.3390/polym11061003

Oliver AL, Oliver A (2017) La nanotecnología, la arquitectura y el arte. Mundo Nano 10(19): 117–128. https://doi.org/10.22201/ceiich.24485691e.2017.19.57719

Pascu B, Ardean C, Davidescu CM, Negrea A, Ciopec M, Duțeanu N, Negrea P, Rusu G (2020) Modified chitosan for silver recovery-kinetics, thermodynamic, and equilibrium studies. Materials 13(3): 657. https://doi.org/10.3390/ma13030657

Pavlova O, Trusova M (2021) Optimisation of conditions for deacetylation of chitin-containing raw materials. Food Sci Technol 15(3): 63–70. https://doi.org/10.15673/fst.v15i3.2152

Petrova YS, Pestov AV, Usoltseva MK, Neudachina LK (2015) Selective adsorption of silver(I) ions over copper(II) ions on a sulfoethyl derivative of chitosan. J Hazard Mater 299: 696–701. https://doi.org/10.1016/j.jhazmat.2015.08.001

Sadiq AC, Rahim NY, Suah FBM (2020) Adsorption and desorption of malachite green by using chitosan-deep eutectic solvents beads. Int J Biol Macromol 164: 3965–3973. https://doi.org/10.1016/j.ijbiomac.2020.09.029

Sergeevna KA, Leonidovna CM, Konstantinovna NL, Sergeevich PI (2020) Method of adsorption-atomic-absorption determination of silver (I) using a modified polysiloxane. React Funct Polym 152: 104596. https://doi.org/10.1016/j.reactfunctpolym.2020.104596

Sharef HY, Fakhre NA (2022) Rapid adsorption of some heavy metals using extracted chitosan anchored with new aldehyde to form a Schiff base. PLoS One 17(9): e0274123. https://doi.org/10.1371/journal.pone.0274123

Soto-Vazquez R, Záyago E, Maldonado LA (2022) Gobernanza de la nanomedicina: Una revisión sistemática. Mundo Nano 15(28): 1e–25e. https://doi.org/10.22201/ceiich.24485691e.2022.28.69682

Sportelli MC, Izzi M, Kukushkina EA, Hossain SI, Picca RA, Ditaranto N, Cioffi N (2020) Can nanotechnology and materials science help the fight against SARS-CoV-2? Nanomaterials (Basel) 10(4): 802. https://doi.org/10.3390/nano10040802

Terzioğlu D, Dalgıç Bozyiğit G, Fırat Ayyıldız M, Chormey DS, Bakırdere S (2021) Combination of slotted quartz tube flame atomic absorption spectrometry and dispersive liquid–liquid microextraction for the trace determination of silver in electroplating rinse bath. Anal Lett 54: 761–771. https://doi.org/10.1080/00032719.2020.1780603

Wang Z, Li Q, Xu L, Ma J, Wei B, An Z, Wu W, Liu S (2020) Silver nanoparticles compromise the development of mouse pubertal mammary glands through disrupting internal estrogen signaling. Nanotoxicology 14(6): 740–756. https://doi.org/10.1080/17435390.2020.1755470

Weißpflog J, Vehlow D, Müller M, Kohn B, Scheler U, Boye S, Schwarz S (2021) Characterization of chitosan with different degree of deacetylation and equal viscosity in dissolved and solid state-Insights by various complimentary methods. Int J Biol Macromol 171: 242–261. https://doi.org/10.1016/j.ijbiomac.2021.01.010

Zhao F, Peydayesh M, Ying Y, Ping J, Mezzenga R (2020) Transition metal dichalcogenide-silk nanofibril membrane for one-step water purification and precious metals recovery. ACS Appl Mater Interfaces 12(21): 24521–24530 https://doi.org/10.1021/acsami.0c07846.

AUTHOR CONTRIBUTION:

Contribution	Jáuregui J	Alvarado AT	Mucha M	Muñoz AM	Chávez H	Molina A	Cuba PA	Melgar EJ	Bolarte M	Mori JA
Concepts or ideas	x	x	x	x	x	x	x	x	x	x
Design	x	x	x	x	x	x	x	x	x	x
Definition of intellectual content	x	x	x	x						
Literature search					x	x	x	x	x	x
Experimental studies	x	x	x	x						
Data acquisition	x		x							
Data analysis	x				x	x	x	x	x	x
Statistical analysis			x							
Manuscript preparation	x	x	x							
Manuscript editing	x	x	x	x						
Manuscript review	x	x	x	x	x	x	x	x	x	x

Citation Format: Jáuregui J, Alvarado AT, Mucha M, Muñoz AM, Chávez H, Molina A, Cuba PA, Melgar EJ, Bolarte M, Mori JA (2023) Bioadsorption of silver ions by calcareous chitin, chitin and chitosan. J Pharm Pharmacogn Res 11(1): 101–109. https://doi.org/10.56499/jppres22.1529_11.1.101